Electronic Supplementary Material (ESI) for Nanoscale.

Supplementary Information

Size-Selective Interaction of Key and Lock Nanocrystals driven by Depletion Attraction at the Nanoscale

D. Hinrichs, R. Himstedt and D. Dorfs

Department of Physical Chemistry and Electrochemistry, Leibniz Universität Hannover, Callinstrasse 3A, 30167 Hannover, Germany

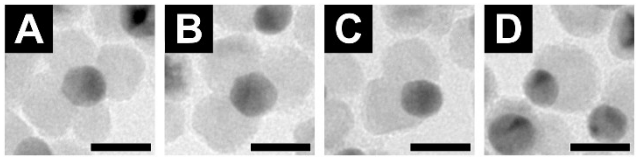

Fig. S1: TEM bright field images of gold-manganese oxide hybrid nanocrystals. Each formed by (A) four, (B) three, (C) two, or (D) one nucleated and fused manganese oxide domains on a single gold domain. The scale bars equal 15 nm.

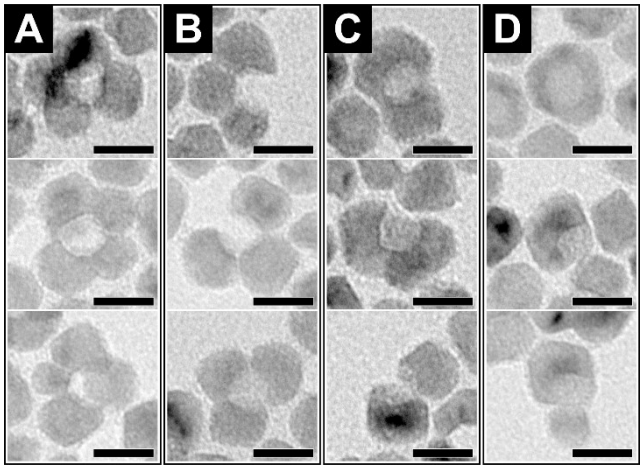

Fig. S2: TEM bright field images of concave manganese oxide nanocrystals (MONCs) obtained with large gold nanocrystals as nucleation seeds. Typically, the structures consist of (A) four, (B) three, (C) two, or (D) one fused crystalline particle domains. Most frequently particles with three or two subdomains can be found in the sample. The scale bars equal 15 nm.

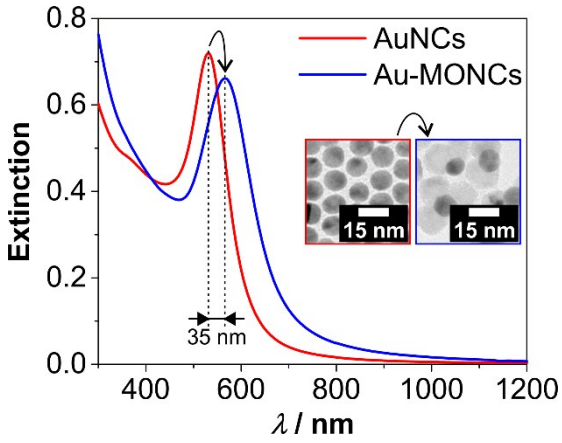

Fig. S3: UV/vis extinction spectra of gold-manganese oxide hybrid nanocrystals (Au-MONCs) and the pristine gold nanocrystals (AuNCs), which were used as seeds for the seed mediated growth to synthesise the Au-MONCs. The colloidal solutions were measured in arbitrary dilutions.

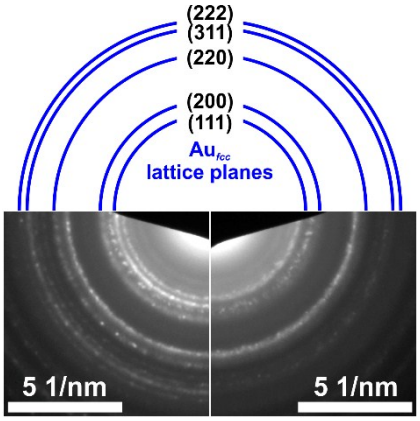

Fig. S4: Ring patterns of selected area electron diffractions of (bottom left) gold-manganese oxide hybrid nanocrystals and (bottom right) concave manganese oxide nanocrystals. For the sake of clarity only the lattice planes for gold were assigned. The manganese oxide is obviously (as discussed in the main article) a mixture of at least two phases (manganosite and pyrolusite) and thereby not unambiguously assignable.

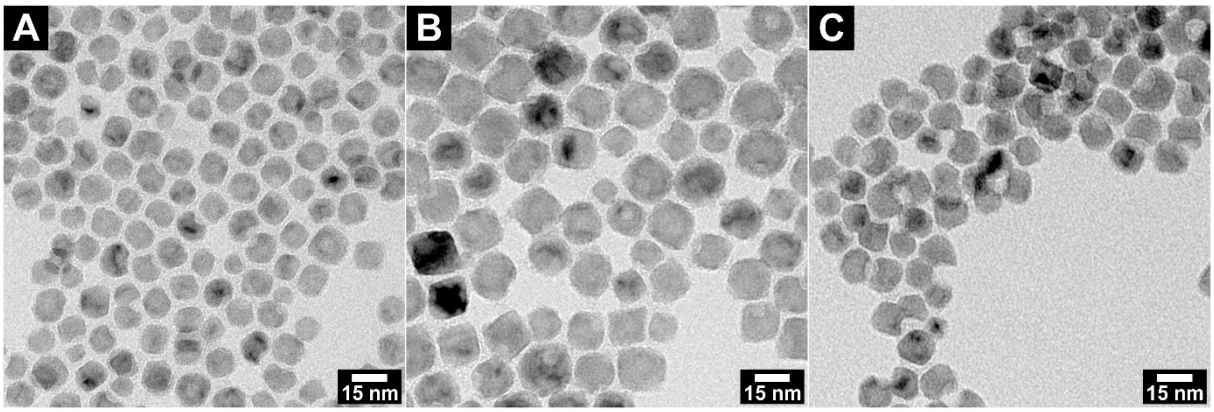

Fig. S5: TEM bright field images of different concave manganese oxide nanocrystals with various void aperture diameters, which are roughly (A) (5.5 ± 0.7) nm, (B) (6.5 ± 0.9) nm, and (C) (9.3 ± 0.9) nm.

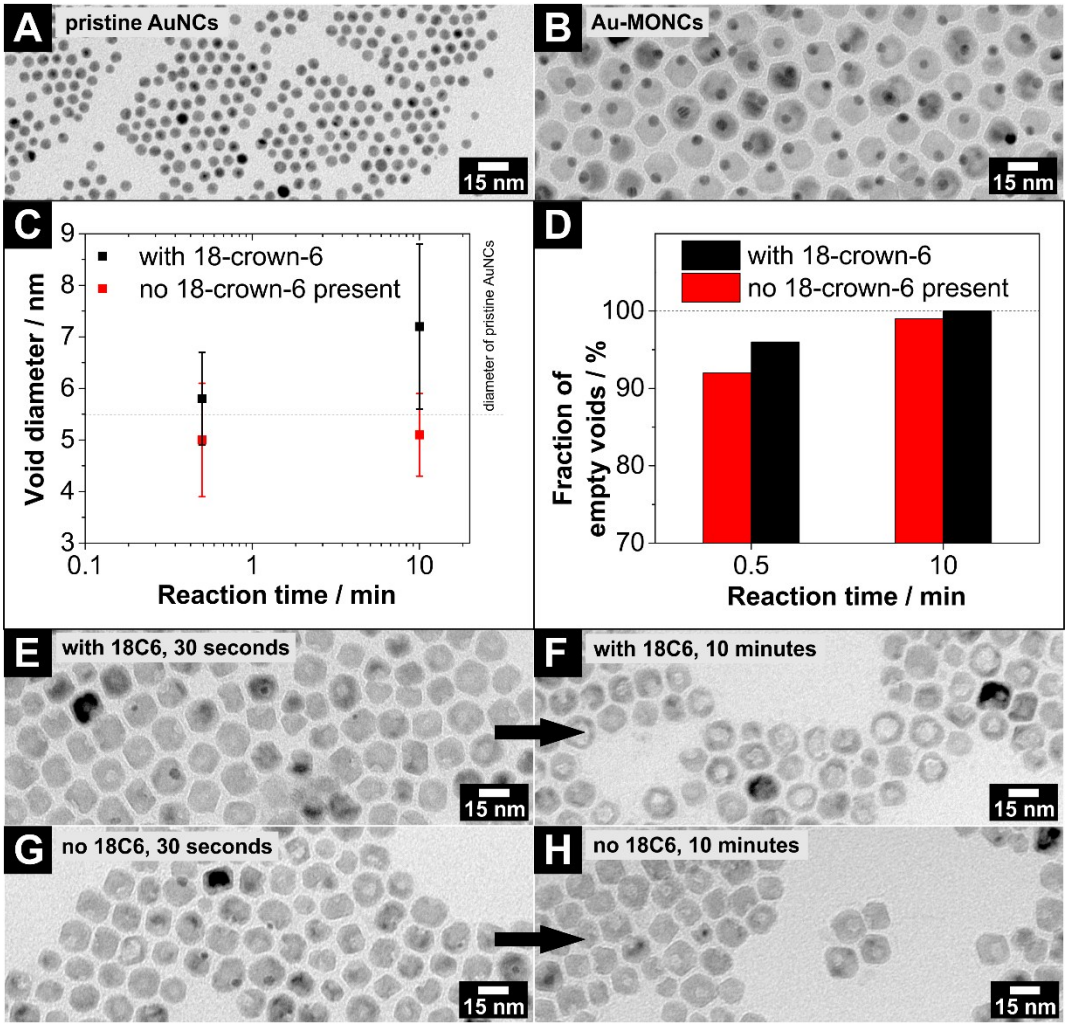

Fig. S6: TEM bright field images of (A) gold nanocrystals (AuNCs) with a diameter of (5.5 ± 0.5) nm, which were used as seeds. (B) The obtained gold-manganese oxide hybrid nanocrystals (MONCs) with a particle diameter of roughly (16.3 ± 1.6) nm, which were used for the following investigation of the etching procedure using potassium cyanide in combination with 18-crown-6-ether (18C6). (C) Diameters of the voids after the etching procedure as a function of the reaction time. Obviously, the void diameter of particles, etched in the presence of 18C6, becomes larger than the initial gold nanocrystal diameter, even after the short reaction time of 30 s. While etching without the addition of 18C6 results in smaller voids than the initial gold nanocrystal diameter. Also, after 10 min reaction time the voids are smaller. (D) Fractions of concave MONCs with empty voids in relation to voids with remaining gold nanoparticles. (E – F) TEM bright field images of potassium cyanide treated MONCs (E and F) in the presence of 18C6, as well as (G and H) without added 18C6.

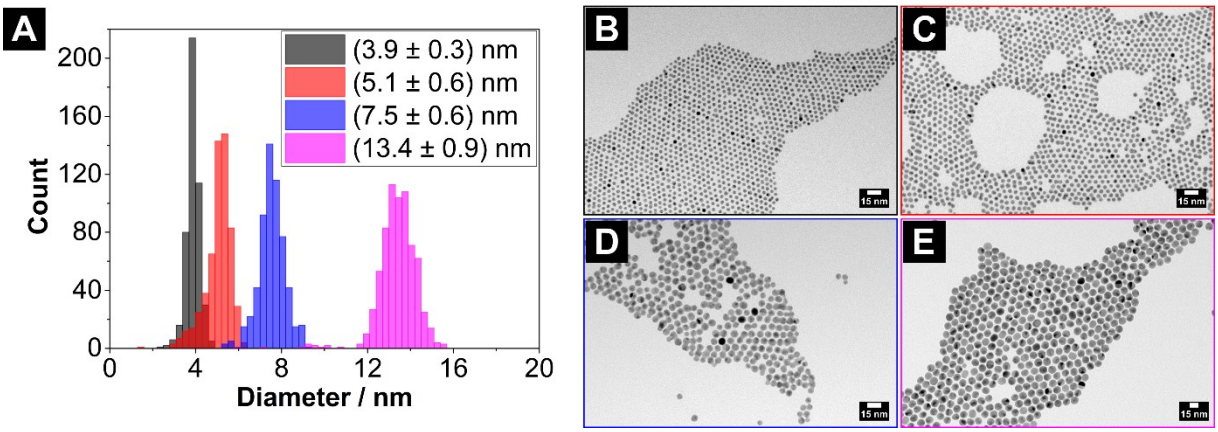

Fig. S7: (A) Histograms of the gold nanocrystal diameters for four differently sized batches. (B – E) Overview TEM bright field images of the highly monodisperse gold nanocrystals with various diameters, which are (B) (3.9 ± 0.3) nm, (C) (5.1 ± 0.6) nm, (D) (7.5 ± 0.6) nm, and (E) (13.4 ± 0.9) nm.

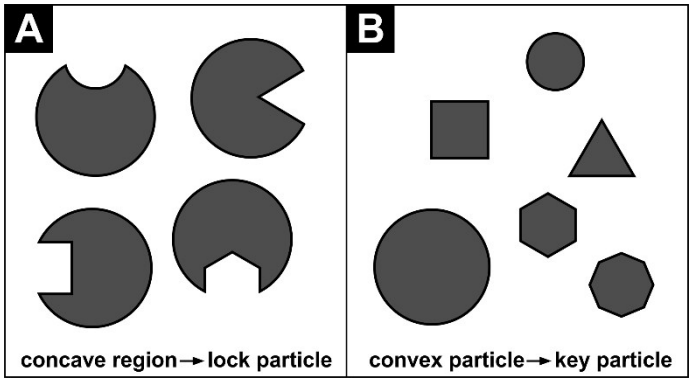

Fig. S8: A scheme to visualize the used definition of the terms *lock particle* and *key particle*. Here, only the particle shape defines the classification. (A) Particles with at least one concave shaped region on their surface are defined as *lock particles*. (B) Particles, which are convex shaped, are defined as *key particles*. It does not matter if the particle surface is spheroidal, kinked, or edged.

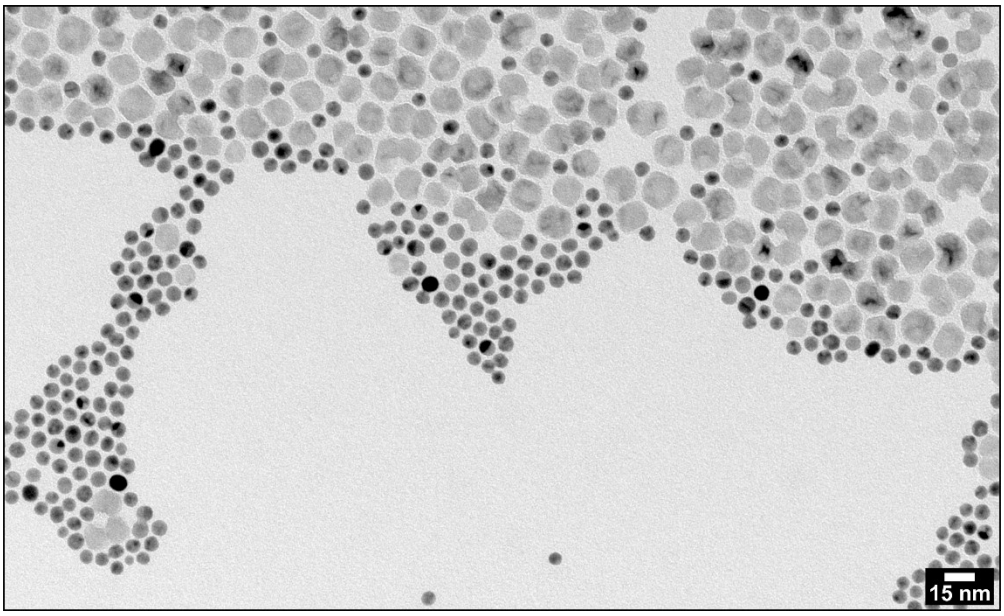

Fig. S9: Overview TEM bright field image taken of a mixture of manganese oxide lock particles and quasi-spherical gold key particles. No depletion agent was added to the system. With inner void diameters of (9.3 ± 0.9) nm and key diameters of (7.5 ± 0.6) nm, the key particles could geometrically fit into the voids of the lock particles. But almost no key-in-lock assemblies can be observed in this system.

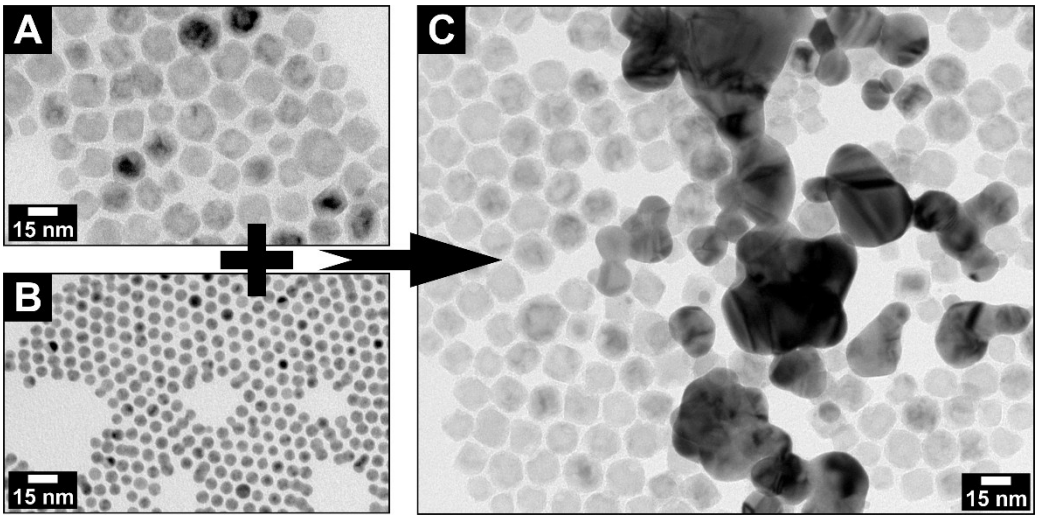

Fig. S10: TEM bright field images of (A) concave manganese oxide nanocrystals with an outer diameter of (17.9 ± 3.3) nm and a void aperture of roughly (6.5 ± 0.9) nm. The particles were not thoroughly cleaned after the iodine treatment. (B) Quasi-spherical gold nanocrystals with (6.1 ± 0.6) nm diameter. (C) A mixture of these particle batches without addition of poly(ethylene glycol) methacrylate (depletion agent) after a few minutes. Almost all gold nanoparticles coalescence to large unspecific-shaped particles. Repeating exactly the same experiment 1 day later with exactly the same particle batches, a stable colloidal solution of completely unchanged pristine nanocrystals is obtained.

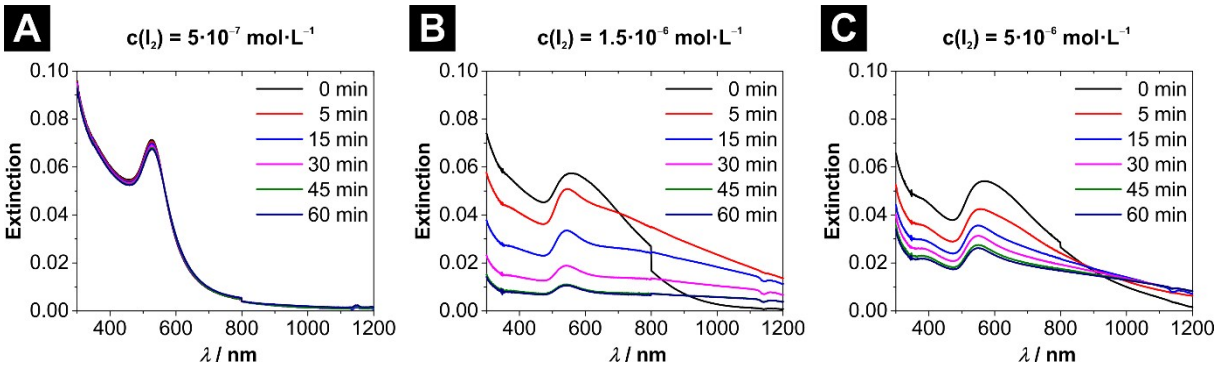

Fig. S11: UV/vis/NIR extinction spectra of pure gold nanocrystals (diameter ≈ 6.2 nm) diluted in toluene (final concentration $2.2 \cdot 10^{-9}$ mol·L^{-1}) with different amounts of added iodine. The final concentrations of iodine in the cuvettes are (A) $5 \cdot 10^{-7}$ mol·L^{-1}, (B) $1.5 \cdot 10^{-6}$ mol·L^{-1}, (C) $5 \cdot 10^{-6}$ mol·L^{-1}. The kink at 800 nm is due to a grating and detector change, which is slower than the coalescence of the AuNCs. The spectra were recorded from 1200 nm to 300 nm with a scanning rate of ≈ 6 nm·s^{-1}.

In experiments with not thoroughly cleaned concave MONCs in combination with pure AuNCs, the AuNCs quickly started to coalescence. The gold forms large polycrystalline and unspecific-shaped particles, with length of up to few hundred nm, see Fig. S10. Thereby we conclude, that residual iodine from the etching step in the synthesis route of concave MONCs can strongly interfere with key-lock experiments. The product in these experiments is similar to the gold destabilisation described by George et al. in their gold-iron oxide system.[1] This effect is irreversible! To proof the direct influence of iodine on the AuNCs, control experiments were conducted. Mixing pure AuNCs solutions with an iodine solution, also results in the fast coalescence of the AuNCs, see Fig. S11. Even a concentration of ≈ 10^{-6} mol·L^{-1} I_2 is enough to force a AuNC colloid of ≈ $2.2 \cdot 10^{-9}$ mole nanocrystals per litre to coalesce. This is a strong proof, that residual iodine can strongly interact with gold nanocrystals and has to be avoided for key-lock experiments by thoroughly washing of the concave MONCs before use.

[1] C. George, D. Dorfs, G. Bertoni, A. Falqui, A. Genovese, T. Pellegrino, A. Roig, A. Quarta, R. Comparelli, M. L. Curri, R. Cingolani, L. Manna, *J. Am. Chem. Soc.*, 2011, **133**, 2205.

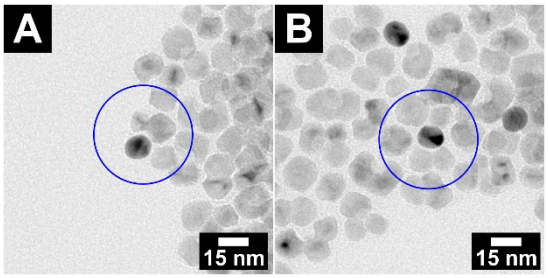

Fig. S12: TEM bright field images of assemblies formed by a manganese oxide nanocrystal (with a very wide void aperture) and a large gold nanocrystal. The blue circles visualise the region of interest.

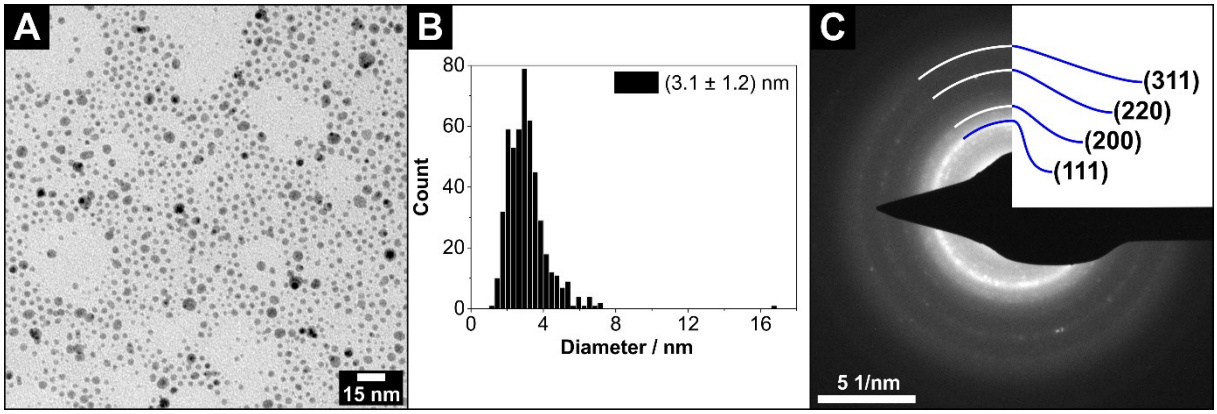

Fig. S13: (A) Overview TEM bright field image of quasi-spherical silver nanocrystals. (B) Size distribution of the nanocrystal diameters, measured from TEM images. A small fraction of particles with diameters larger than 15 nm are present. (C) Selected area electron diffraction of the silver nanocrystals with assigned lattice planes for silver.

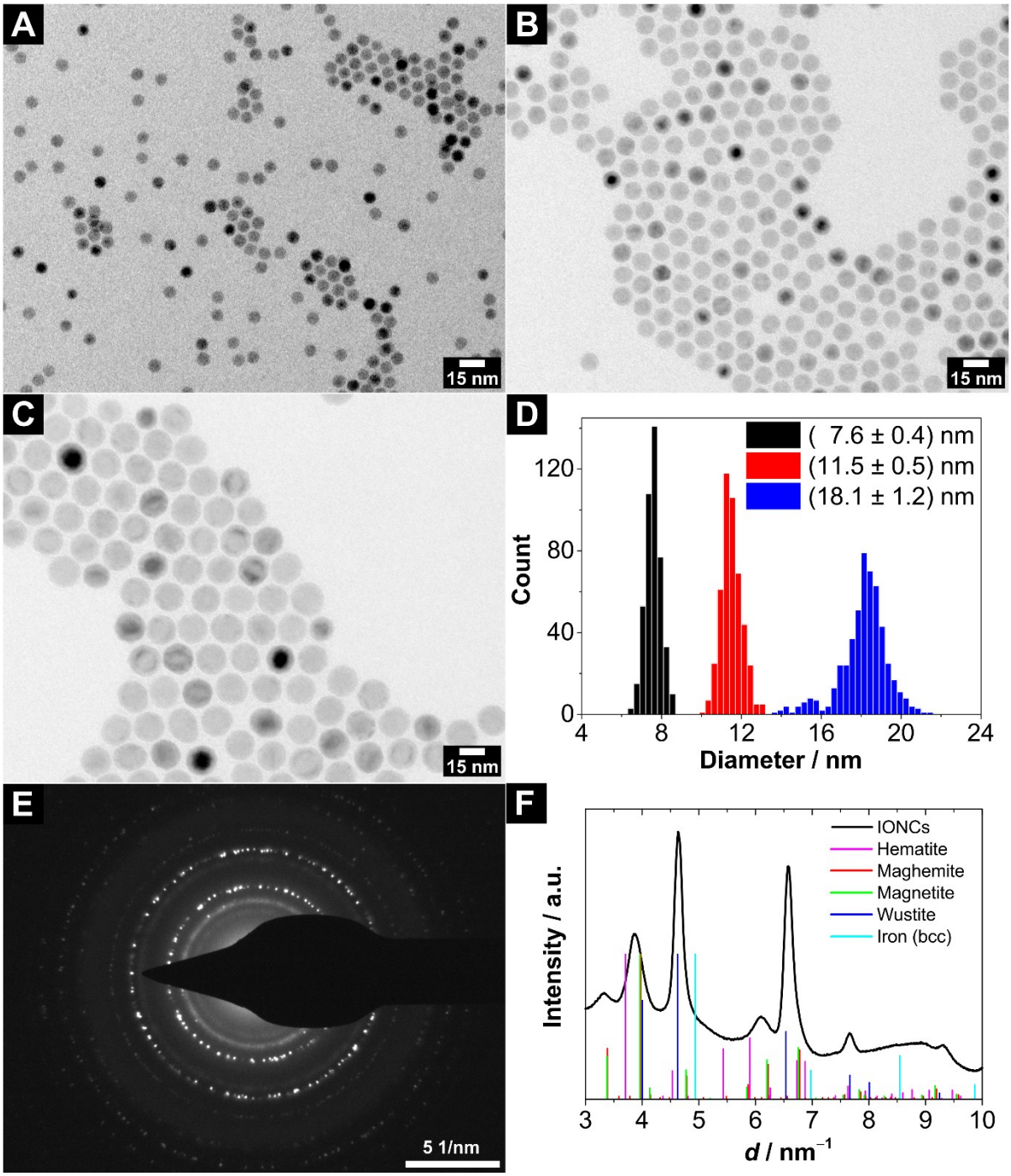

Fig. S14: (A – C) Overview TEM bright field images of iron oxide nanocrystals (IONCs) of various particle diameters, which are (A) (7.6 ± 0.4) nm, (B) (11.5 ± 0.5) nm, and (C) (18.1 ± 1.2) nm. (D) Size distributions of the nanocrystal diameters, measured from TEM images. (E) Selected area electron diffraction (SAED) of the iron oxide nanocrystals. Iron oxide nanocrystals with 18.1 nm in diameter were used for higher intensities of reflections. (F) A plot of the azimuthal integrated intensity of the SAED in dependence of the reciprocal lattice plane distances. The reference structural data show the reflection positions displayed as vertical lines. The positions were calculated from the XRD data of hematite (rhombohedral Fe_2O_3, PDF card #: 01-071-5088), maghemite (cubic γ-Fe_2O_3, PDF card #: 00-039-1346), magnetite (cubic Fe_3O_4, PDF card #:01-071-6336), wustite (cubic FeO, PDF card #: 01-089-0687), and iron (*bcc*-Fe, PDF card #: 00-006-0696). Obviously, the IONCs are a mixture of different phases.

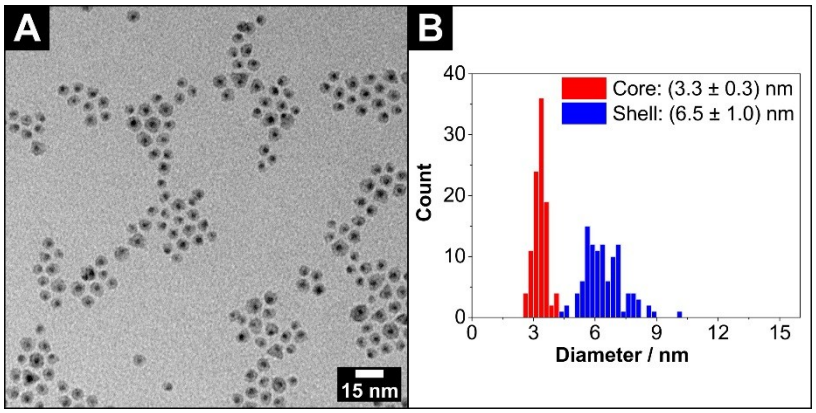

Fig. S15: (A) Overview TEM bright field image of gold-nickel sulfide core-shell nanocrystals. (B) Size distributions of the gold core and nickel sulfide shell diameters measured from TEM images.